



CHORUS

This is the accepted manuscript made available via CHORUS. The article has been published as:

Diffusion-limited encounter rate in a three-dimensional lattice of connected compartments studied by Brownian-dynamics simulations

Ran Li and Brian A. Todd

Phys. Rev. E **91**, 032801 — Published 4 March 2015

DOI: [10.1103/PhysRevE.91.032801](https://doi.org/10.1103/PhysRevE.91.032801)

Diffusion-Limited Encounter Rate in a Three-dimensional Lattice of Connected Compartments Studied by Brownian Dynamics Simulations

Ran Li

*School of Electrical and Computer Engineering and
Department of Physics and Astronomy, Purdue University.*

Brian A. Todd*

Department of Physics and Astronomy, Purdue University.

Abstract

We considered the rate at which a diffusing particle encounters a target in a three-dimensional lattice of compartments with semi-permeable walls. This work expands a previous theory [Phys. Rev. Lett. **113**, 028303 (2014)] for the encounter rate in the dilute limit of targets to the general case of any density of targets. We also used Brownian dynamics (BD) simulations to evaluate the approximations in the analytical theory. We find that the largest errors in the analytical theory are on the order of 10%. This work therefore demonstrates an analytical theory capable of describing the encounter rates in compartmentalized environments for any level of confinement and any target density.

PACS numbers: 82.20.Uv 83.10.Mj 87.15.H-

* batodd@purdue.edu

I. INTRODUCTION

In many cases of practical interest, diffusion occurs through a liquid phase containing a field of less mobile obstacles. The most straightforward examples include porous catalysts[1] and rocks[2] but a similar physical picture also applies to diffusion in some biological environments.[3–5] Key features of all of these systems are a strong attenuation of the diffusion coefficient when the size of a diffusing particle approaches the pore size [6–10] and a variable diffusion coefficient at length-scales less than the pore size.[6–20] This latter property—the decrease in diffusion coefficient with increasing length—is often referred to as “anomalous sub-diffusion”. [21, 22]

Theories for transport in porous materials are relatively well developed. One of the simplest models capable of describing the local confinement present in porous materials involves a periodic lattice of semipermeable barriers that retard, but do not forbid, the passage of a diffusing particle.[23] We favor this particular underlying model because it isolates the physical effect of local confinement from other factors such as the detailed physical interactions between the diffusing particle and the obstacles. For a lattice of semipermeable compartments, it is possible to obtain a simple analytical expression relating the microscopic properties of the compartments to diffusion at large length scales.[24]

While transport in compartmentalized environments is relatively well studied, the effects of confinement on diffusion-limited encounter rates are less well developed. Klann et al. found that the diffusion-limited reactions sense an intermediate diffusion coefficient amongst the spectrum of anomalous diffusion coefficients.[25] Guigas et al. showed by simulations that anomalous sub-diffusion increases the probability of two nearby reactants encountering one another.[26] Haugh compared two different models of anomalous sub-diffusion and found that there are only subtle differences between the two models.[27]

We recently obtained an analytical expression for the diffusion-limited encounter rate in compartmentalized environments.[24] We used the “Wiener sausage” approach [28, 29] to find the volume of space contacted by a particle undergoing anomalous sub-diffusion in an environment containing compartments. The Wiener sausage volume refers to the volume of space contacted by a sphere whose time dependent position is a Wiener process, i.e. a continuous time random walk. Each time the Wiener sausage volume increases by the average volume containing one reactant, the diffusing particle encounters, on average, one

reactant. Hence, the rate of increase of the Wiener sausage volume is the diffusion-limited encounter rate.

In this paper, we describe the diffusion-limited encounter rate in a three-dimensional system of connect compartments. We generalize our previous work on diffusion-limited encounter rates in the dilute limit of targets to any density of targets.[24] We also use Brownian dynamics (BD) simulation to check approximations in the analytical theory. We find that the deviations do not strongly affect the average rates predicted by our theory. This work therefore shows that the analytical theory presented can predict the diffusion limited encounter rate for any scale of confinement and any density of targets.

II. PROBLEM STATEMENT

We characterize the average time required for a single Brownian particle diffusing in an infinite cubic lattice of compartments to encounter a target (Fig. 1). The walls of each compartment are semipermeable and impede movement of the particle between compartments. Targets are randomly distributed with number density n per compartment. An encounter occurs when the separation between the Brownian particle and a target is less than a distance R , termed the “reaction radius” or “capture radius”.

Diffusion within a compartment is characterized by diffusion coefficient D_0 . The compartment has size a and permeability of the walls \mathcal{P} . \mathcal{P} quantifies the difficulty with which the diffusing particle crosses a compartment wall. Infinite permeability is equivalent to no compartments and zero permeability means that the particle cannot pass a compartment wall. The diffusion coefficient observed at scales much larger than a is given by Crick’s formula, [23, 30]

$$\frac{D}{D_0} = \frac{1}{1 + (\mathcal{P}a)^{-1}}. \quad (1)$$

Hence, once the compartment size a has been determined, either D or \mathcal{P} can be chosen to describe the level of confinement. We use D because it is typically the more experimentally accessible parameter.

This problem contains one arbitrary length and one arbitrary time scale. We remove these two parameters by non-dimensionalizing all other quantities by a common length and/or time scale. Throughout, we use the Latin alphabet for dimensional quantities and Greek letters to denote non-dimensionalized quantities.

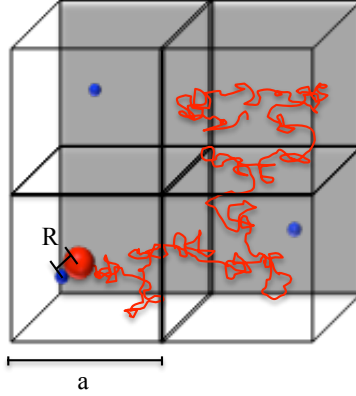


FIG. 1. (color online) We characterize the average time required for a Brownian particle (red, large) diffusing in an infinite three-dimensional cubic lattice of semi-permeable compartments to encounter a target (blue, small). For clarity, the cartoon shows only four compartments but it is meant to depict an infinite three-dimensional lattice.

All lengths are defined relative to the characteristic radius of compartment, L . L is defined as the radius of a sphere with same volume as the compartment with size a , $L = (\frac{3}{4\pi})^{\frac{1}{3}}a$. All times are relative to the transit time across a compartment $t_0 = L^2/D_0$. In this reduced form there are three parameters that completely specify the system: the relative reaction radius $\rho = R/L$, the relative diffusion coefficient $\delta = D/D_0$, and the target density n .

To obtain predictions for a particular reaction, our results need only be scaled by these quantities. For instance, β -enolase has a hydrodynamic radius of about 4 nm and diffusion coefficient in buffer $D_0 = 56 \mu\text{m}^2\text{s}^{-1}$. The diffusion coefficient in the cytosol of muscle cells is reduced to $D = 13.5 \mu\text{m}^2\text{s}^{-1}$. [31] Assume that the muscle cell has characteristic radius of $L = 25 \text{ nm}$ (the typical values for the intracellular environment are $L = 10 - 50 \text{ nm}$ [10, 32–37]). In Fig. 5, the simulation result shows that for $\delta = 0.2$ (red curve), the relative reaction rate is ~ 1.2 at a target density $n = 0.5$ per compartment. This concentration of targets corresponds to $C = n/N_A v_c = 0.025\text{M}$, where N_A is the Avogadro constant and $v_c = 4/3\pi L^3$ is the volume of the compartment. With $t_0 = 6.7 \mu\text{s}$, the reaction rate constant needs to be scaled by $n/(Ct_0) = 3 \times 10^6 \text{ s}^{-1}\text{M}^{-1}$, resulting a predicted reaction rate constant of $3.6 \times 10^6 \text{ s}^{-1}\text{M}^{-1}$.

III. ANALYTICAL THEORY

A. Dilute Limit of Targets

This section is a brief recapitulation of the analytical theory for the encounter rate in the dilute limit of targets from Ref.[24]. Only the key assumptions in the analytical theory are highlighted below as they will be tested in this paper using BD simulations. For a complete derivation of the results in this Section, please refer to Ref.[24].

The encounter rate constant in the dilute limit is,

$$k = \lim_{t \rightarrow \infty} \frac{V(t)}{t}, \quad (2)$$

where $V(t)$ is the Wiener sausage volume. The average rate of increase of the Wiener sausage volume, $V(t)/t$ can be obtained as the product of the rate of moving between compartments, s , and the average increase in Wiener sausage volume for an *isolated* compartment. s depends on the compartment topology. For instance, for a cubic lattice, $s = 6D/a^2$. The analytical solutions developed here are intended to be useful approximations for poorly defined compartment topologies that are encountered in experimental work. In this case, the exact relationship between D and the mean lifetime would likely be unknown. We chose the relation $s = 3D/L^2$ because it has the correct scaling, is similar to the exact results for well-defined compartment topologies (such as the cubic lattice), and leads to compact results for the reaction rate. We denote the Wiener sausage volume in an isolated compartment as $v(t)$. In order to calculate an average value, we assume that the compartment residence times, Δt follow an exponential distribution,

$$p(\Delta t) \sim s e^{-s\Delta t}. \quad (3)$$

Equation 3 is only an approximate expression for the residence time distribution and we evaluate the deviations from Eq. 3 using Brownian dynamics simulations in Section V A 1. We also assume that the Wiener sausage volume in an isolated compartment follows an exponential rise to the full search of the compartment volume,

$$v(\Delta t) \sim v_c (1 - e^{-\Delta t/\tau_c}), \quad (4)$$

where v_c is the compartment volume and τ_c is the characteristic time constant. τ_c describes the time required to reduced the unsearched fraction of the compartment volume by a factor

of e^{-1} . Equation 4 is only an approximate expression for the Wiener sausage volume as a function of time and we evaluate the quality of this approximation using Brownian dynamics simulations in Section V A 2. Under these assumptions, an analytical solution to Eq. 2 is, [24]

$$\frac{k}{k_0} = \frac{x}{x\zeta + 1} \left(1 - P_R + P_R \frac{x\zeta}{x\zeta + 1} \right), \quad (5)$$

where k is the encounter rate in the dilute limit, $k_0 = 4\pi D_0 R$ is Smoluchowski's diffusion limit, and P_R is the probability of a particle returning to a compartment.[38] Eq. 5 depends on two dimensionless parameters: $x = DL/D_0R$, the dominant scaling variable and ζ given by,

$$\zeta = \frac{1}{2} - \rho + \sqrt{\frac{1}{4} - \rho P_R}. \quad (6)$$

$\zeta \rightarrow 1$ as $\rho \rightarrow 0$, whereby x becomes the sole parameter governing diffusion-limited encounter rates.

B. Limit of Many Targets

In the dilute limit of targets, the diffusing particle needs to cross a compartment wall in order to encounter a target. As the density of targets increases, it becomes increasingly likely that the diffusing particle will start off in a compartment that contains at least one target. Since confinement tends to restrict the diffusing particle to the compartment, it is possible that the particle encounters one of these targets without ever crossing a compartment wall. This leads to different reaction kinetics than in the dilute limit.

In the extreme limit of many targets per compartment, the diffusing particle almost certainly encounters a target without ever crossing the compartment wall. In this case, a compartment behaves as an isolated reaction vessel. Diffusion occurs only within the compartment with diffusion coefficient D_0 , the encounter rate is $k_0 = 4\pi D_0 R$, and the average time to the first encounter is $\tau_s = 1/ik_0$, where i is the number of targets initially present in the compartment. To determine the average encounter time in this limit, we enumerate all of the different possible starting configurations and calculate the appropriate expectation value for τ_s , the time for a purely intra-compartmental encounter. We use the subscript s to denote the short time encounter process that occurs without crossing a compartment barrier.

Let $P(i)$ be the probability that, in an environment with average density n targets, there are i targets initially present in a compartment. This probability is given by the Poisson distribution,

$$P(i) = \frac{n^i}{i!} e^{-n}. \quad (7)$$

$P(s | i)$ is the conditional probability that an encounter occurs inside a compartment given that there are initially i targets present. We can again construct this probability from sampling statistics.

For a target that occupies volume R^3 , the compartment contains $N = L^3/R^3$ volume elements that could contain a target. It takes a time $R^2/3D_0$ to move a distance R . So, within the average time the particle remains in the compartment, $L^2/3D$, the particle will move between volume elements $M = L^2D_0/R^2D$ times. The probability of finding one of the i targets from N volume elements after M attempts is,

$$P(s | i) = 1 - \left(\frac{N-i}{N} \right)^M. \quad (8)$$

It is simple to show that $M/N = x^{-1}$ and in the limit of $N \rightarrow \infty$,

$$P(s | i) = 1 - e^{-i/x}. \quad (9)$$

In the limit of many targets, the diffusing particle almost certainly encounters a target without crossing a compartment wall. In this case, we can neglect reactions that require the particle to cross a compartment boundary and the expectation value of the encounter time for the short processes is given by,

$$\langle \tau_s \rangle = \sum_{i=0}^{\infty} P(s | i) P(i) \tau_s(i). \quad (10)$$

C. Intermediate Density of Targets

For an intermediate density of targets, an encounter may occur through a short process where the particle encounters a target present in its initial compartment. Or, an encounter may occur through a long process whereby the particle needs to cross a compartment wall. We assume that the average encounter time for the intermediate density of targets is the weighted sum of the long processes and the short processes averaged over all possible starting configurations.

$$\langle \tau \rangle = \sum_{i=0}^{\infty} P(i) (P(s | i) \tau_s(i) + (1 - P(s | i)) \tau_l). \quad (11)$$

$\tau_l = 1/nk$ is the time for the long process and $\tau_s = 1/ik_0$ is the time for the short process. Inserting and rearranging, we have

$$\frac{\langle \tau \rangle}{\tau_l} = 1 + \sum_{i=0}^{\infty} P(i)P(s | i) \left(\frac{nk}{ik_0} - 1 \right). \quad (12)$$

For $n \ll 1$, the probability of having more than 1 target in a compartment is small. In this case, the summation can be truncated after $i = 1$. Additionally, $P(1)$ can be approximated as n , giving

$$\frac{\langle \tau \rangle}{\tau_l} \sim 1 - n(1 - e^{-1/x}). \quad (13)$$

This equation expresses the fact that for a compartmentalized environment with $x < 1$, the average encounter rate acquires a dependence on target density that is not present in the absence of confinement.

IV. BROWNIAN DYNAMICS (BD) SIMULATION

A. BD for Free Diffusion

BD simulations numerically integrate a stochastic differential equation forward in time to create trajectories of Brownian particles. For free diffusion without inertia, the time-stepping equation for a Brownian particle between τ and $\tau + \Delta\tau$ in a three-dimensional space is given by

$$\vec{\chi}(\tau + \Delta\tau) = \vec{\chi}(\tau) + \sqrt{2\Delta\tau}\vec{\xi}. \quad (14)$$

Each component of $\vec{\xi}$ is a Gaussian random variable with $\langle \xi(t) \rangle = 0$ and $\langle \xi(t_1)\xi(t_2) \rangle = \delta(t_1 - t_2)$. Both $\vec{\chi}$ and $\Delta\tau$ are dimensionless quantities as defined previously.

B. BD in Cubic Lattice of Compartments

In the compartment interior, the particle diffuses using BD identical to free diffusion. However, if the particle attempts to cross a compartment wall, the step is subject to reflection about the plane defined by the compartment wall with a probability P_b . The probability P_b is the direct indication of the compartment permeability, and is calculated according to Eq. 8.4 in Ref. [23] as

$$P_b = \frac{1 + \mathcal{P}\lambda}{1 + 2\mathcal{P}\lambda}, \quad (15)$$

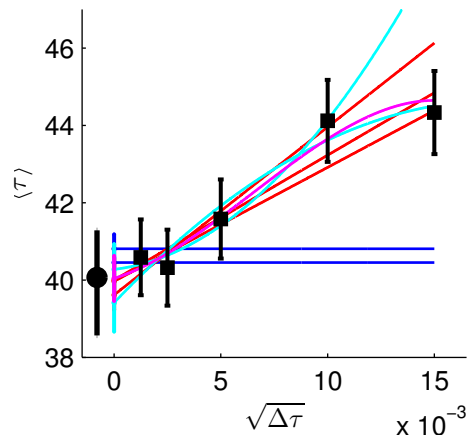


FIG. 2. (color online) Extrapolating discrete time Brownian Dynamics simulations to the continuum limit. Mean encounter times are obtained at 5 different values of the simulation time step (black squares). The values are then fitted to all possible over-determined non decreasing polynomials to obtain intercepts at $\Delta\tau = 0$. This process is repeated by iteratively removing the largest time step until only the two smallest time steps remained in the extrapolation. The mean encounter time at the continuum limit is then the mean of all extrapolations and the associated uncertainty are the union of the uncertainties of all extrapolations. This mean value and its uncertainty are plotted as the black dot with error bar slightly offset from 0 for clarity. The extrapolation polynomials of order zero, one, two and three are plotted as colored lines.

where $\lambda = \pi\sqrt{\Delta\tau}/4$ is the mean step size for the Gaussian random steps.

C. Encounter Rate

Each simulation is initiated by creating a field of randomly distributed targets and a single randomly placed particle. The particle diffuses with time step $\Delta\tau$ until it encounters a target. The time required to encounter a target τ_i is one realization of the diffusion-limited encounter time. This procedure is repeated for at least 4000 times to obtain a mean encounter time, $\langle \tau \rangle$.

D. Extrapolations

The mean time required for a particle to encounter a target, $\langle\tau\rangle$, simulated by Brownian dynamics, has a prominent dependence on the simulation time step $\Delta\tau$.^[39] To recover a continuum limit, we conducted simulations with five different time steps and then extrapolated the finite steps to $\Delta\tau = 0$ (shown in Fig. 2). The extrapolation method is modified from the algorithm originally described by Ottinger.^[40] We fitted $\langle\tau\rangle$ vs. $\sqrt{\Delta\tau}$ to all possible over-determined non decreasing polynomial and accepted all statistically reasonable fits. The encounter time at the continuum limit was then the mean of all accepted extrapolations and the associated uncertainty was the union of the uncertainties of all accepted extrapolations. Taking the union of all uncertainties results is a conservative estimate for the uncertainty in our simulated encounter times.

Mean diffusion-limited encounter times, $\langle\tau\rangle$ at different values of the simulation time step $\Delta\tau$ are plotted in Fig. 2 as black squares with error bars representing standard error of the mean. Each point is the mean of at least 4000 independent simulations. To obtain the continuum limit, we fitted $\langle\tau\rangle$ vs. $\sqrt{\Delta\tau}$ to all possible over-determined non decreasing polynomials (e.g. for 5 points, polynomials of order 3 and below), as described by Ottinger.^[40] Any fit with a chi-squared probability value greater than 0.1 was accepted.^[41] We then remove the simulation with largest $\Delta\tau$ from the series and repeat the fitting (with maximum polynomial order reduced by 1). This process is repeated until only the simulations with the two smallest $\Delta\tau$ remain. The accept fits are plotted for polynomials of order zero (dark blue lines), one (red lines), two (cyan lines), and three (magenta lines). The extrapolations to $\Delta\tau = 0$ are simply the zero-order terms in each fitted polynomial (symbols at $\Delta\tau = 0$). The uncertainties are the square roots of the zero order terms in each covariance matrix (error bars at $\Delta\tau = 0$).

The aggregate mean for all extrapolations (black dot, slightly offset from $\Delta\tau = 0$ for clarity) and the 95% confidence interval of the aggregate probability density (bold black error bar) define the continuum limit of the average encounter time and associated uncertainty. Because the 95% confidence interval is sensitive to the tails of the distribution, this procedure produces error bars that are essentially the union of the uncertainties of all extrapolations. These fits essentially represent all statistically reasonable description of the relationship between $\langle\tau\rangle$ and $\Delta\tau$. This procedure is used to extrapolate each encounter rate in all

related calculations.

The example shown here is for a density of one target per 50 compartments, $\rho = 0.16$, and $\delta = 1$. Because $\delta = 1$ represents no confinement, we expect the continuum limit of these simulations to be equal to the Smoluchowski diffusion limit, $50 / (4\pi \times 0.1) \sim 39.79$.

E. Exit Time in an Isolated sphere

In developing the theory for dilute limit of targets, we assume that the distribution of the exit time in an isolated sphere is similar to the exponential distribution, as specified by Eq. 3. We examined the probability distribution of the exit time in an isolated sphere using BD simulations and compared the results with Eq. 3.

In order to calculate an exit time, the diffusing particle starts off at a random location and diffuses inside the sphere using BD. We define that the particle has exited the compartment when the distance between the center of the particle and the center of the sphere is larger than the characteristic radius L . The distribution of exit times was calculated from at least 10^4 samples.

F. Wiener Sausage Volume

The analytical theory for the dilute limit of targets was derived under the assumption that the Wiener sausage volume in an isolated compartment $v(\Delta t)$ grows as specified by Eq. 4. To our knowledge, there is no analytical theory for the Wiener sausage volume in a finite domain. Thus we carried out a BD simulation to check this assumption.

A random trajectory of the diffusing particle was first generated up to time τ using BD, $\vec{\chi}(\tau)$. The Wiener sausage volume is the volume of space that is within a distance ρ of any point in $\vec{\chi}(\tau)$,

$$v(t) = \int I(\vec{\chi}(t), \vec{\chi}'(t)) d\vec{\chi}'^3, \quad (16)$$

where I is the indicator function defined as

$$I(\vec{\chi}(t), \vec{\chi}'(t)) = \begin{cases} 1, & \text{if } |\vec{\chi}(t) - \vec{\chi}'(t)| \leq R \\ 0, & \text{otherwise.} \end{cases}$$

We evaluated this integral using Monte Carlo integration. Twenty independent trajectories were then generated and the Wiener sausage volume were averaged.

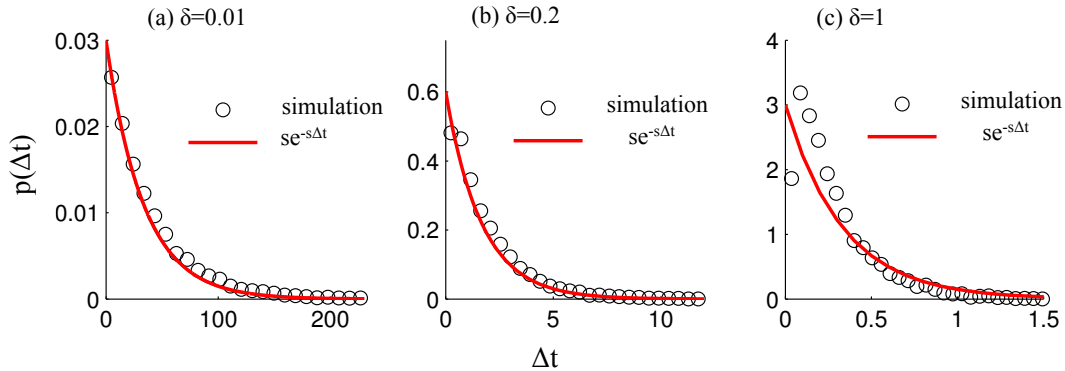


FIG. 3. (color online) The probability density of exit times from a compartment with semipermeable walls. The probability densities calculated using BD simulation (black circles) are plotted together with the probability density $se^{-s\Delta t}$ (red curves). Simulations were conducted with three relative diffusion coefficients, $\delta = 0.01$, $\delta = 0.2$ and $\delta = 1$ for (a), (b), and (c), respectively.

G. Computations

The BD simulations were run on 200 cores in parallel on BoilerGrid, a distributed computing system running HTCondor operated by Rosen Center for Advanced Computing at Purdue University over a period of several months.

V. RESULTS

A. Properties of Isolated Compartment

Two properties of a compartment that influence the rate of increase in the Wiener sausage volume in the dilute limit are (1) the average time that a diffusing particle spends in a compartment before exiting and (2) the average increase in Wiener sausage volume during its residence (see Eq. 2). In order to obtain an analytical solution, we approximated the distribution of exit times with Eq. 3, and we approximate the increase in Wiener sausage volume with Eq. 4. In the next two sections, we evaluated these two approximations with BD simulations.

1. Probability Density of the Exit Time

In developing the theory of encounter rates for the dilute limit of targets, one assumption made is that the distribution of exit times is similar to an exponential distribution (specified by Eq. 3). We numerically calculated exit times using BD simulations and compared the simulated distribution to the exponential distribution, Eq. 3.

The exit time is defined as the time required for a particle placed randomly within a compartment to pass through the compartment wall. Exit times were simulated with three different levels of confinement specified by three relative diffusion coefficients, $\delta = 0.01$, $\delta = 0.2$ and $\delta = 1$, respectively. Each of the probability densities were calculated from at least 10^4 samples. The simulated probability densities are plotted as black circles in Fig. 3. The exponential function specified by Eq. 3 is plotted as red curves alongside for comparison.

With very strong confinement ($\delta = 0.01$), the most probable exit time is small compared to the average exit time. For this case, the probability distribution resembles the exponential distribution specified by Eq. 3 where the most probable exit time is 0 (in Fig. 3(a), the black circles match the red curve). As the confinement weakens ($\delta = 0.1$ and $\delta = 1$), the average exit time becomes smaller and it can be seen that the most probable exit times in the BD simulations are non-zero. This simply reflects the fact that a randomly placed particle requires a finite time to diffuse to a compartment wall. For these highly permeable cases, the exit time distribution deviates from the exponential distribution. $\delta = 1$ is the limit of a completely permeable compartment so Fig. 3(c) represents the largest possible difference between the actual exit time distribution and the exponential distribution.

At $\delta = 1$, although the shape of the the simulated distribution deviates from the exponential distribution, the simulated distribution has a similar first moment to the exponential distribution (the mean of the exponential distribution is 0.33 and the mean of the simulated exit times is 0.28). In the analytical theory, we used the exit time probability density to calculate the expectation value of the Wiener sausage volume, $v(\Delta t) = v_c(1 - e^{-\Delta t/\tau_c})$ (Eq. 4). Δt has an average value of $\langle \Delta t \rangle = 1/s = L^2/3D$, whereas $\tau_c = L^3/3D_0R$. Because Δt is smaller than τ_c , $\langle \Delta t \rangle/\tau_c \sim R/L \ll 1$, we can approximate $v(\Delta t)$ over the non-zero part of the probability density for Δt by the first order term of its Taylor expansion about $\Delta t = 0$,

$$v(\Delta t) = v_c(1 - e^{-\Delta t/\tau_c}) \sim \frac{v_c}{\tau_c} \Delta t \quad (17)$$

Because $v(\Delta t)$ is linear with respect to Δt , any probability density with the correct first

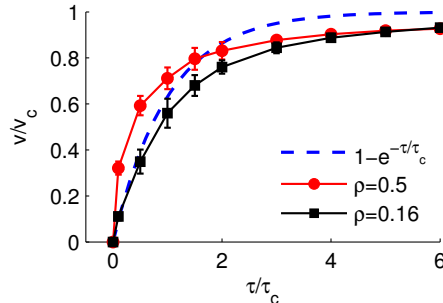


FIG. 4. (color online) The Wiener sausage volume in an isolated impermeable sphere as a function of time. The Wiener sausage volume $v(t)$ is normalized by the sphere volume $v_c = \frac{4}{3}\pi L^3$. Time is normalized by the time constant τ_c (see Eq. 4). The symbols are simulation results for $\rho = 0.5$ (red dots) and $\rho = 0.16$ (black squares). The dashed line is Eq. 4.

moment will give the same expectation value for $v(\Delta t)$,

$$\langle v \rangle = \int \rho(\Delta t) v(\Delta t) d\Delta t \quad (18)$$

$$\sim \frac{v_c}{\tau_c} \int \rho(\Delta t) \Delta t d\Delta t \quad (19)$$

$$\sim \frac{v_c}{\tau_c} \langle \Delta t \rangle. \quad (20)$$

Hence, even for $\delta = 1$, where the probability density function differs from the exponential, the expectation value calculated with respect to the exponential will be similar to its actual expectation value.

2. Wiener Sausage Volume

The analytical theory for the encounter rate in the dilute limit described in section III A is based on the assumption that the Wiener sausage volume in an isolated compartment $v(\Delta t)$ evolves in time as described by Eq. 4. We used BD simulations to check this assumption. At time 0, a particle with size ρ was placed randomly inside a spherical compartment of unit radius. Then a Brownian trajectory is evolved using Eq. 14 inside the sphere. The sphere is impermeable such that the diffusing particle is reflected back when it attempts to step outside the boundary. The Wiener sausage volume for the diffusing particle trajectory was calculated according to Eq. 16 using Monte Carlo integration. This process was repeated 20 times, starting from random locations, and the Wiener sausage volumes for each trajectory

were averaged to obtain symbols shown in Fig. 4. The error bars represent the standard errors of the mean.

The numerical results are shown in Fig. 4 with Wiener sausage volume, $v(t)$ normalized by the compartment volume, v_c . The simulation time is normalized by the time constant, τ_c in Eq. 4. Simulations were obtained with two different relative reaction radii, $\rho = 0.16$ (black squares) and $\rho = 0.5$ (red dots). The exponential increase assumed by Eq. 4 is plotted as the blue dashed line for comparison.

For $\rho = 0.16$, the initial increase in the Wiener sausage volume is indistinguishable from Eq. 4 (in Fig. 4, black squares overlap the blue dashed line for $\tau/\tau_c < 1$). As time increases, Eq. 4 approaches a limiting value of $v/v_c = 1$ exponentially. Around $\tau/\tau_c \sim 1$, the simulations begin to deviate below Eq. 4 and approaches the limiting value of $v/v_c = 1$ more slowly. The slower approach to the limiting value in the simulations is due to an excluded volume effect; the probability for a particle to touch a region of space is lower near the boundary of the compartment, as compared to the compartment interior. As τ/τ_c becomes large, nearly all of the space in the sphere that is not yet in the Wiener sausage volume is adjacent to the walls of the sphere. A particle can only touch a region of space adjacent to the boundary tangentially, whereas a point in the compartment interior can be contacted by any point within the particle. The improbability of precisely placing the particle in tangential contact with the boundary of the compartment causes the limiting approach to complete search of the compartments to be slower in the BD simulations than predicted by Eq. 4.

For $\rho = 0.5$, the simulated Wiener sausage volume initially increases more rapidly than predicted by Eq. 4 (in Fig. 4, the red dots are above blue line for $\tau/\tau_c < 1$). The rapid increase in the Wiener sausage volume observed in the simulations is caused by the initial placement of a particle into a completely unexplored compartment. Thus, at $\tau/\tau_c = 0$ the Wiener sausage volume increased discontinuously by $v/v_c = \rho^3$. This discontinuity is not captured by Eq. 4. At longer times, the simulated Wiener sausage volume makes a slower approach to the limiting value of $v/v_c = 1$ than predicted by Eq. 4 (red dots below blue line at $\tau/\tau_c > 2$). This is caused by the same excluded volume effect as described above for $\rho = 0.16$.

A compartment must be larger than the particle it contains. Consequently, $\rho = 0.5$ represents an extreme case. Yet, even for $\rho = 0.5$, the time dependence for the Wiener

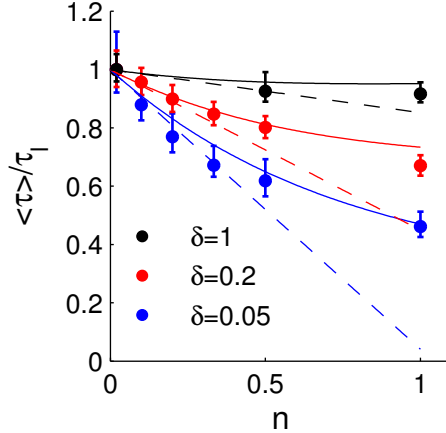


FIG. 5. (color online) The normalized average encounter time as a function of target density. The average encounter time $\langle \tau \rangle$ combining both short and long processes is normalized by the encounter time for the dilute limit. The black (uppermost), red (middle) and blue (bottom) dots are the BD simulation data for $\delta = 1$, $\delta = 0.2$ and $\delta = 0.05$, respectively. The solid lines are the predictions from Eq. 12 and the dashed lines are predictions from Eq. 13.

sausage volume is approximately described by Eq. 4; namely, the time constant τ_c captures the scale over which the Wiener sausage volume changes by a factor e^{-1} . In Fig. 4, $v/v_c = e^{-1}$ at $\tau/\tau_c \sim 0.7$ for red dots, i.e. similar to the predicated $\tau/\tau_c = 1$. For $\rho < 0.5$, the discontinuous increase in initial volume and the excluded volume at the boundary will be smaller and the increase in the Wiener sausage volume will more closely match the exponential, Eq. 4.

B. Effect of Finite Target Density

When many targets are present, it is possible that the particle encounters a target within its initial compartment without ever crossing a compartment wall. This leads to different encounter time than in the dilute limit. In section III C, we expanded the previous theory developed in the dilute limit of targets[24] to the case of finite density of targets. Here, we use BD simulations to check the analytical theory.

Simulated encounter rates as a function of number density of targets per compartment n are shown in Fig. 5 as symbols. The simulated encounter rates were calculated using BD simulations in a cubic lattice as described in Section IV. A Brownian particle was placed

randomly inside a cubic lattice with target density n . The particle underwent diffusion until encountering a target. The process was repeated at least 4000 times with different random starting conditions and the encounter times were averaged to obtain $\langle\tau\rangle$. The average encounter time is normalized by the encounter time at $n = 1/50$, τ_l , which approximates the infinitely dilute limit. $\langle\tau\rangle/\tau_l$ therefore represents the encounter rate relative to the infinitely dilute limit. Simulations were performed at different levels of confinement at $\delta = 0.05$ (blue dots, bottom), $\delta = 0.2$ (red dots, middle) and $\delta = 1$ (black dots, uppermost), while keeping the relative reaction radius constant at $\rho = 0.16$.

The solid lines are predictions from Eq. 12, and the dashed lines are predictions from Eq. 13. For all three different levels of confinement ($\delta = 1$, $\delta = 0.2$ and $\delta = 0.05$), there is no significant difference between the simulated encounter time and the predictions from Eq. 12 (in Fig. 5, all three solid curves can describe simulated data). The largest discrepancy, $\sim 10\%$, occurs at $n = 1$, $\delta = 0.2$. The simplified expression Eq. 13 is accurate for $n < 0.2$ (dash lines). For $n > 0.2$, Eq. 13 underestimates the encounter time. This deviation is caused by making the simplification that the time scale for the short process is sufficiently small to be considered 0.

VI. DISCUSSION

We considered the rate at which a diffusing particle encounters a target in a three-dimensional lattice of compartments with semi-permeable walls. Expanding on a previous work that gave an analytical expression for the encounter rate in the dilute limit of targets, we have developed a theory that can now describe any density of targets (i.e. Eq. 12). The largest discrepancy between our theory and the BD simulations is $\sim 10\%$. We have also used BD simulations to probe the most difficult limits of parameter space for the approximations in the analytical theory and found that, where deviations exist (i.e. Fig. 3(c)), they do not strongly affect the average rates predicted by our theory. This work therefore demonstrates an analytical theory capable of describing the diffusion-limit for encounter rates in compartmentalized environments for any value of the compartment confinement and any target density.

The compartmentalized environment that we consider is perhaps the simplest physical system that exhibits a length-scale dependent diffusion coefficient; within a compartment,

a rapid, unencumbered diffusion predominates, whereas, diffusion between compartments is slower due to the impediments imposed by a compartment wall. This “anomalous sub-diffusion” is characteristic of diffusion in, for instance, biological environments where local diffusion is similar to diffusion in water[14, 37, 42–44] but translational diffusion over distances > 100 nm is 3-100 fold slower than diffusion in water. [6–20] Because anomalous sub-diffusion is common to many real environments, we expect our analytical results to provide more appropriate predictions of diffusion-limited encounter rates than the classic Smoluchowski diffusion limit.

The theory that we described here makes a number of predictions that can be observed in experiments and that are qualitatively different from the traditional Smoluchowski diffusion-limit, $k = 4\pi DR$. Namely, Smoluchowski’s Eq. predicts that the encounter rate is proportional to the diffusion-coefficient. In compartmentalized environments, the coupling between the encounter rate and the diffusion coefficient can be much weaker. Indeed, whenever $x > 1$, i.e. $D/D_0 > R/L$ we expect that the encounter rate will be weakly affected by decreases in the diffusion coefficient. This may explain why reaction rates recently measured inside living cells were similar to those measured *in vitro*, despite an expected 5-fold decrease in the diffusion coefficient. [45]

A yet stronger signature of the effects described here would be the dependence of the relative encounter rate, k/k_0 on a single dominant scaling variable, $x = DL/D_0R$. Thus, for any compartmentalized environment—with any values of the parameters D , D_0 , L , and, R —we expect the relative encounter rate not to depend on the parameters individually but solely through their combination in the dimensionless number x . It may be possible to systematically test this prediction by engineering, for example, porous structures or gels with different pore sizes and checking whether k/k_0 vs. x describes a single universal curve, as described by Eq. 5. Alternately, as more biological reactions are studied *in vivo*, we expect the reaction rate constants will fall on the single universal curve described by Eq. 5.

An additional signature of confinement is the change in the encounter rate “constant” as the target density approaches one target per compartment (section III C). In this regime, the average encounter time decreases relative to the encounter time for the dilute limit (see Eq. 12 and Fig. 5). This effect is caused by the high probability for an encounter to occur whenever a reaction is initiated with a diffusing particle and a target within the same compartment. This dependence of the encounter rate constant on target density is a clear

indication of the role of confinement on the encounter rate. The change in the encounter time is again governed solely by the dimensionless variable x , according to Eq. 13. Hence, a measured change in reaction rate at $n \geq 1$ for $x < 1$ would be a clear signature of the role of the confinement.

Our work has only focused on how local confinement affects diffusion-limited encounter rates. We have not included a number of other potentially important effects including hydrodynamic interactions between the diffusing particle and the compartment walls and variability in compartment properties. Consideration of the interplay of all these effects is a subject for future work.

VII. CONCLUSION

In this paper, we describe the rate at which a diffusing particle encounters a randomly placed target in a three-dimensional system of connected compartments with semi-permeable walls. This work expands our previous theory for the encounter rate in the dilute limit of targets to the general case of any density of targets. We also used BD simulations to numerically check approximations needed in order to obtain analytical solutions. For highly permeable compartments, the exponential distribution of residence times assumed by our theory is violated. However, the average rate depends primarily on the first moment of the distribution which is accurately described by the exponential distribution. This paper therefore demonstrates an analytical theory that is capable of describing the encounter rates in compartmentalized environments for any level of confinement and any target density.

ACKNOWLEDGMENTS

This work was supported by a grant from the Division of Materials Research of the National Science Foundation(1006485-DMR).

-
- [1] U. Pasaogullari and C. Y. Wang, *Electrochim. Acta* **49**, 4359 (2004).
 - [2] T. B. Boving and P. Grathwohl, *Journal of Contaminant Hydrology* **53**, 85 (2001).
 - [3] S. B. Zimmerman and A. P. Minton, *Annu. Rev. Biophys. Biomol. Struct.* **22**, 27 (1993).

- [4] R. J. Ellis, Trends Biochem. Sci. **26**, 597 (2001).
- [5] A. P. Minton, J. Cell Sci. **119**, 2863 (2006).
- [6] S. Popov and M. M. Poo, J Neurosci **12**, 77 (1992).
- [7] K. Luby-Phelps, P. E. Castle, D. L. Taylor, and F. Lanni, Proc Natl Acad Sci U S A **84**, 4910 (1987).
- [8] M. Arrio-Dupont, S. Cribier, G. Foucault, P. F. Devaux, and A. d'Albis, Biophys J **70**, 2327 (1996).
- [9] O. Seksek, J. Biwersi, and A. S. Verkman, J Cell Biol **138**, 131 (1997).
- [10] J. A. Dix and A. S. Verkman, Annu. Rev. Biophys. **37**, 247 (2008).
- [11] M. B. Elowitz, M. G. Surette, P. E. Wolf, J. B. Stock, and S. Leibler, J Bacteriol **181**, 197 (1999).
- [12] M. C. Konopka, K. A. Sochacki, B. P. Bratton, I. A. Shkel, M. T. Record, and J. C. Weisshaar, J Bacteriol **191**, 231 (2009).
- [13] C. W. Mullineaux, A. Nenninger, N. Ray, and C. Robinson, J Bacteriol **188**, 3442 (2006).
- [14] M. J. Dayel, E. F. Y. Hom, and A. S. Verkman, Biophys. J. **76**, 2843 (1999).
- [15] A. Partikian, B. Olveczky, R. Swaminathan, Y. Li, and A. S. Verkman, J Cell Biol **140**, 821 (1998).
- [16] G. Meacci, J. Ries, E. Fischer-Friedrich, N. Kahya, P. Schwille, and K. Kruse, Phys Biol **3**, 255 (2006).
- [17] K. M. Slade, R. Baker, M. Chua, N. L. Thompson, and G. J. Pielak, Biochemistry **48**, 5083 (2009).
- [18] R. P. Kulkarni, M. Bak-Maier, and S. E. Fraser, Proc Natl Acad Sci U S A **104**, 1207 (2007).
- [19] J. Chen and J. Irudayaraj, ACS Nano **3**, 4071 (2009).
- [20] J. W. Wojcieszyn, R. A. Schlegel, E. S. Wu, and K. A. Jacobson, Proc Natl Acad Sci U S A **78**, 4407 (1981).
- [21] J. P. Bouchaud and A. Georges, Physics Reports-review Section of Physics Letters **195**, 127 (1990).
- [22] S. Havlin and D. Benavraham, Advances In Physics **36**, 695 (1987).
- [23] J. G. Powles, M. J. D. Mallett, G. Rickayzen, and W. A. B. Evans, Proc. R. Soc. Lond. A **436**, 391 (1992).
- [24] R. Li, J. A. Fowler, and B. A. Todd, Phys. Rev. Lett. **113** (2014).

- [25] M. T. Klann, A. Lapin, and M. Reuss, *BMC Syst. Biol.* **5**, 71 (2011).
- [26] G. Guigas and M. Weiss, *Biophys. J.* **94**, 90 (2008).
- [27] J. M. Haugh, *Biophys J* **97**, 435 (2009).
- [28] A. M. Berezhkovskii, Y. A. Makhnovskii, and R. A. Suris, *J. Stat. Phys* **57**, 333 (1989).
- [29] A. M. Berezhkovskii and G. H. Weiss, *Phys. Rev. E* **54**, 92 (1996).
- [30] F. Crick, *Nature* **225**, 420 (1970).
- [31] M. ArrioDupont, G. Foucault, M. Vacher, A. Douhou, and S. Cribier, *Biophys. J.* **73**, 2667 (1997).
- [32] Y. Lill, W. A. Kaserer, S. M. Newton, M. Lill, P. E. Klebba, and K. Ritchie, *Phys. Rev. E* **86**, 021907 (2012).
- [33] G.-W. Li, O. G. Berg, and J. Elf, *Nature Physics* **5**, 294 (2009).
- [34] R. Swaminathan, S. Bicknese, N. Periasamy, and A. S. Verkman, *Biophys. J.* **71**, 1140 (1996).
- [35] S. Papadopoulos, K. D. Jurgens, and G. Gros, *Biophys. J.* **79**, 2084 (2000).
- [36] A. S. Verkman, *Trends Biochem. Sci.* **27**, 27 (2002).
- [37] K. Luby-Phelps, *Int. Rev. Cytol.* **192**, 189 (2000).
- [38] M. Koiwa and S. Ishioka, *J. Stat. Phys.* **30**, 477 (1983).
- [39] T. Barenbrug, E. Peters, and J. Schieber, *J. Chem. Phys.* **117**, 9202 (2002).
- [40] H. Ottinger, *Stochastic Processes in Polymer Fluids* (Springer, Berlin, 1996).
- [41] W. Press, S. Teukolsky, W. Vetterling, and B. Flannery, *Numerical Recipes in C, The Art of Scientific Computing*, 2nd ed. (Cambridge, 1992).
- [42] K. Fushimi and A. S. Verkman, *J. Cell Biol.* **112**, 719 (1991).
- [43] N. Periasamy, M. Armijo, and A. S. Verkman, *Biochemistry* **30**, 11836 (1991).
- [44] R. Swaminathan, C. P. Hoang, and A. S. Verkman, *Biophys. J.* **72**, 1900 (1997).
- [45] Y. Phillip, V. Kiss, and G. Schreiber, *Proc. Nat. Acad. Sci. USA* **109**, 1461 (2012).